Supplementary Information

Water Jacket Systems for Temperature Control of Petri Dish Cell Culture Chambers

Samira Uharek [1,2], Sara Baratchi [3], Jiu Yang Zhu [4], Majed Ali Alshehri [4], Arnan Mitchell [4], Karsten Rebner [2], Christian Karnutsch [1,*] and Khashayar Khoshmanesh [4,*]

[1] Institute for Sensor- and Information Systems (ISIS), Research Group 'Integrated Optofluidics and Nanophotonics (IONAS)', University of Applied Sciences Karlsruhe, 76133 Karlsruhe, Germany; samira.uharek@gmx.de

[2] Department of Applied Chemistry, Reutlingen University, Reutlingen, 72762 Baden-Wuerttemberg, Germany; karsten.rebner@reutlingen-university.de

[3] School of Health and Biomedical Sciences, RMIT University, Melbourne 3083, Victoria, Australia; sara.baratchi@rmit.edu.au

[4] School of Engineering, RMIT University, Melbourne 3001, Victoria, Australia; toro.zhujiuyang@yahoo.com.au (J.Y.Z.); alqushairi.majed@gmail.com (M.A.A.); arnan.mitchell@rmit.edu.au (A.M.)

* Correspondence: christian.karnutsch@hs-karlsruhe.de (C.K.); khashayar.khoshmanesh@rmit.edu.au (K.K.)

Received: 19 January 2019; Accepted: 8 February 2019; Published: date

Supplementary Information 1: Prototype water jacket used for experimental measurements

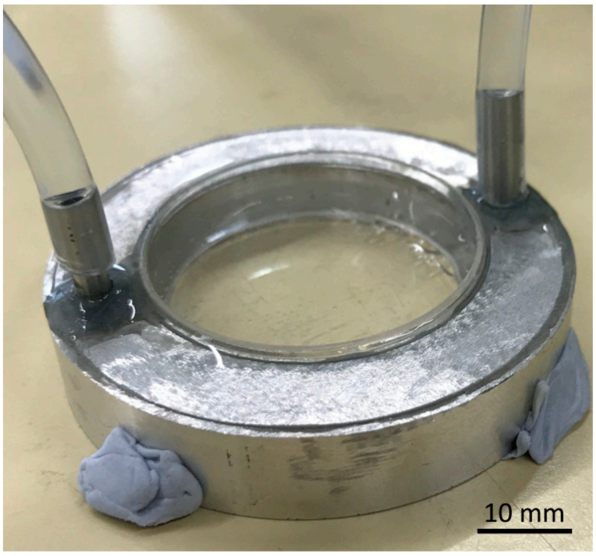

Figure S1. Prototype water jacket used for measuring the temperature profile across the top free surface of the Petri dish using an infrared camera.

Supplementary Information 2: Thermo-physical properties of the materials used in numerical simulations

Table S1. Thermo-physical properties of the materials used in numerical simulations

Property	Symbol	Value
Density (kg/m^3)	ρ_{water}	998
	ρ_{jacket}	2719
	ρ_{sample}	998
	$\rho_{Petri\ dish}$	1020
	ρ_{washer}	2100
Dynamic viscosity (Pa.s)	μ_{water}	0.001
Heat capacity (J/kg.K)	$c_{p\ water}$	4182
	$c_{p\ jacket}$	871
	$c_{p\ sample}$	4182
	$c_{p\ Petri\ dish}$	1400
	$c_{p\ washer}$	1175
Thermal conductivity (W/mK)	k_{water}	0.6
	k_{jacket}	202
	k_{sample}	0.6
	$k_{Petri\ dish}$	0.3
	k_{washer}	0.2
Air temperature (°C)	T_{air}	22
Free convection coefficient (W/m^2K)	h_{air}	10

Supplementary Information 3: Effect of water flow rate

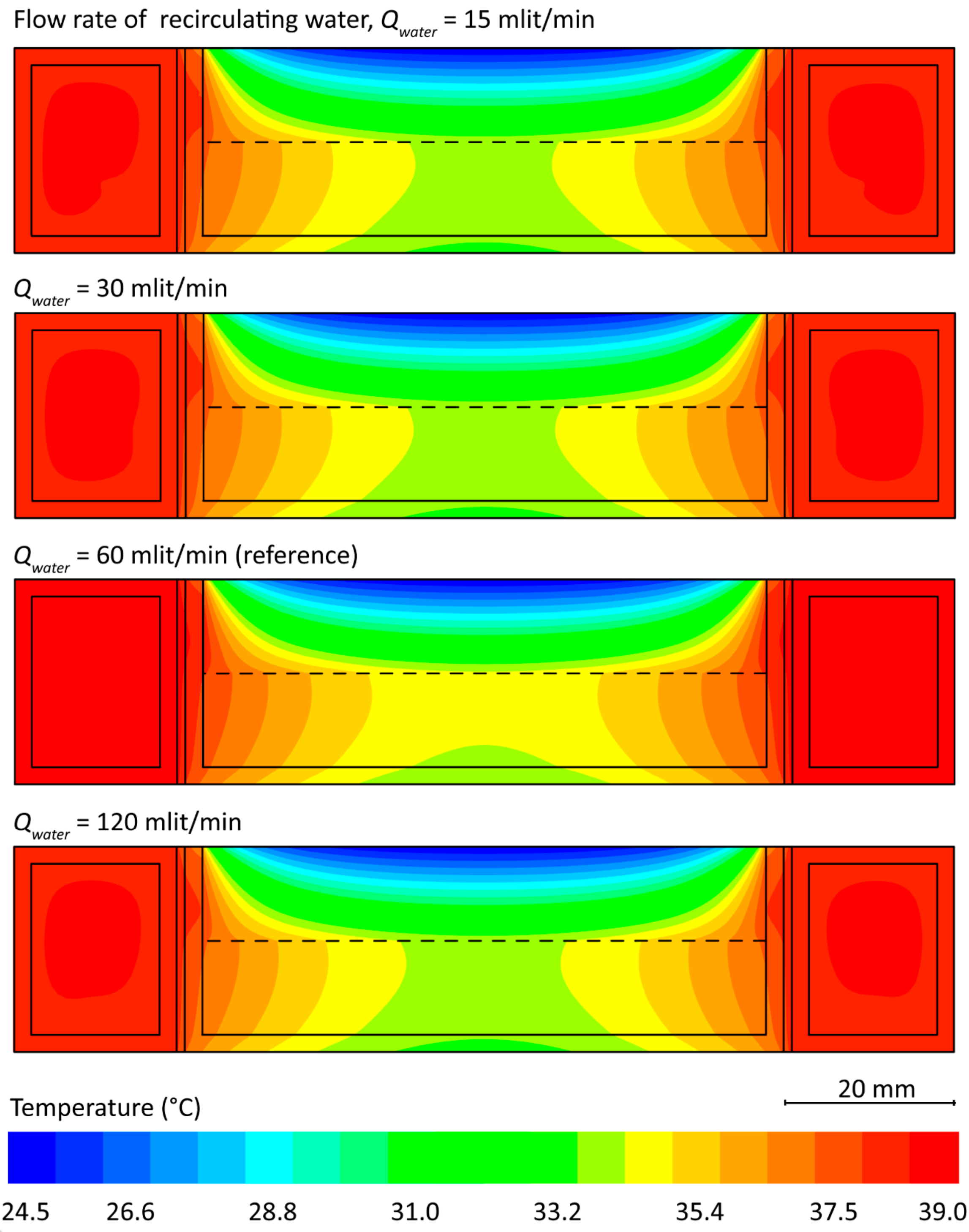

Figure S2. Characterizing the thermal performance of the water jacket system with respect to the flow rate of the water recirculating through the water jacket (Q_{water}). The above contours show the temperature distribution along the middle cross section of the Petri dish for Q_{water} values of 15, 30, 60 and 120 mL/min, as discussed in **Figure 3a**.

Supplementary Information 4: Effect of water temperature

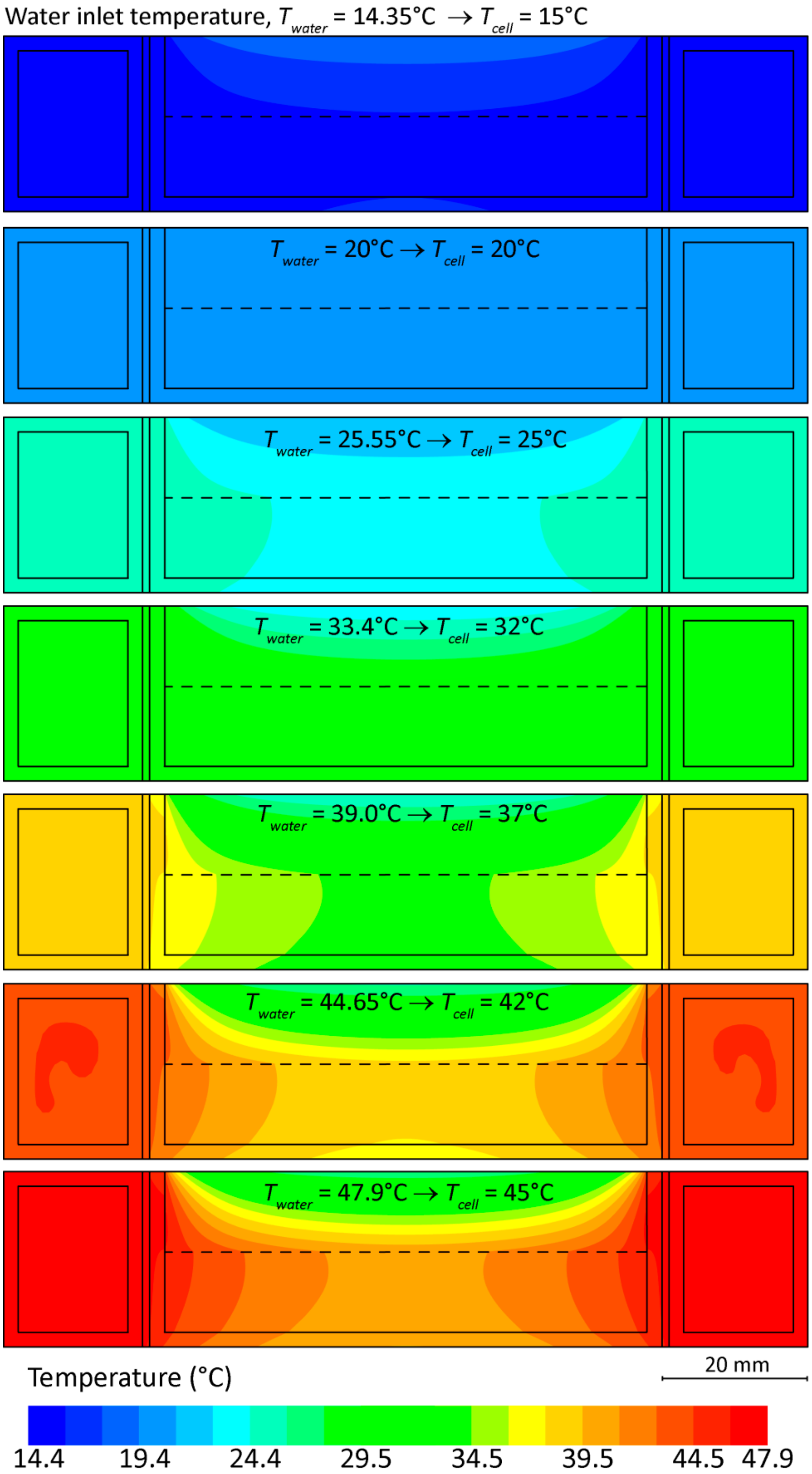

Figure S3. Characterizing the thermal performance of the water jacket system with respect to the temperature of the water entering the water jacket (T_{water}). The above contours show the temperature distribution along the middle cross section of the Petri dish for T_{water} values of 14.35, 20, 25.55, 33.4, 39, 44.65 and 47.9°C, as discussed in **Figure 3b**.

Supplementary Information 5: Effect of air temperature

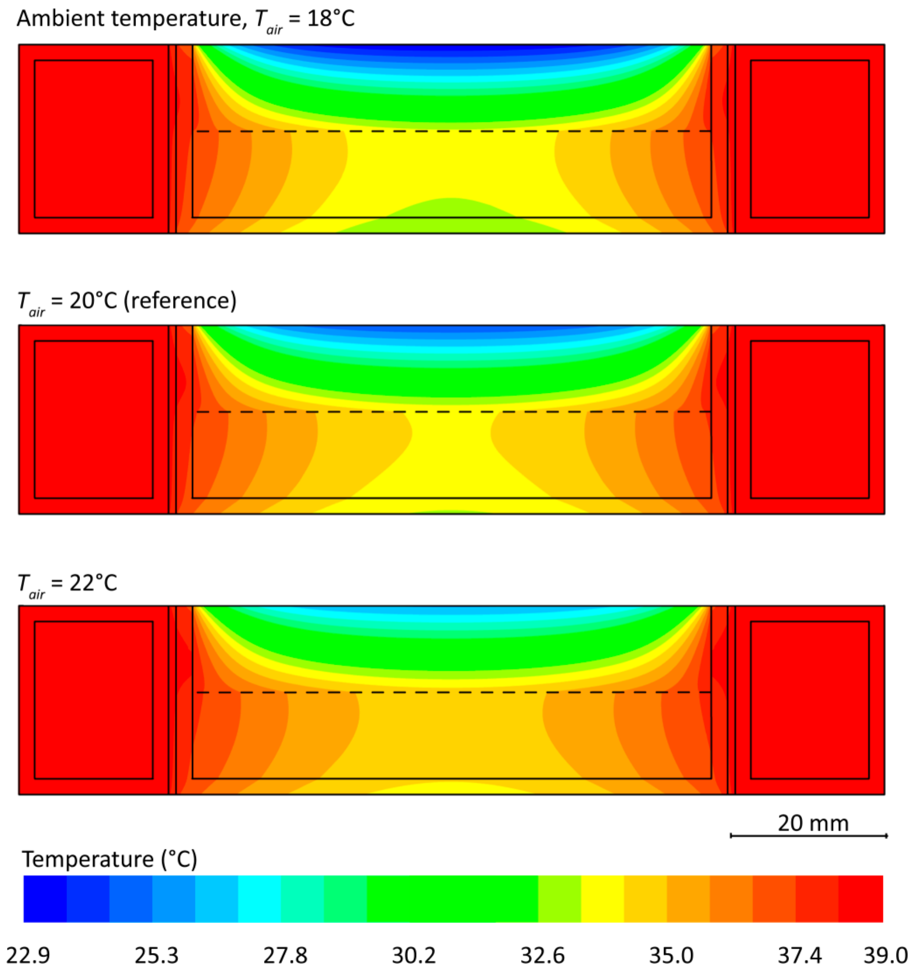

Figure S4. Characterizing the thermal performance of the water jacket system with respect to the temperature of the ambient air (T_{air}). The above contours show the temperature distribution along the middle cross section of the Petri dish for T_{air} values of 18, 20 and 22°C, as discussed in **Figure 3c**.

Supplementary Information 6: Effect of air convection coefficient

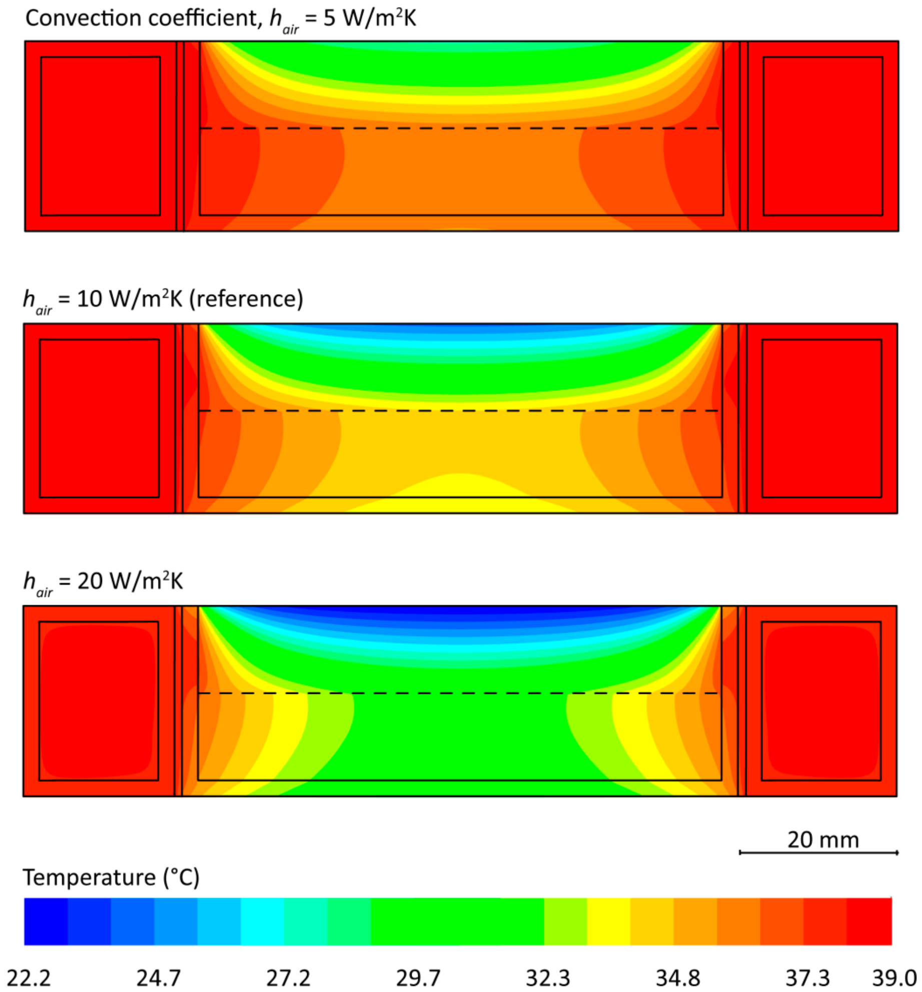

Figure S5. Characterizing the thermal performance of the water jacket system with respect to the convective heat transfer coefficient of ambient (h_{air}). The above contours show the temperature distribution along the middle cross section of the Petri dish for h_{air} values of 5, 10, and 20 W/m^{2}K, as discussed in **Figure 3d.**

Supplementary Information 7: Effect of Petri dish diameter

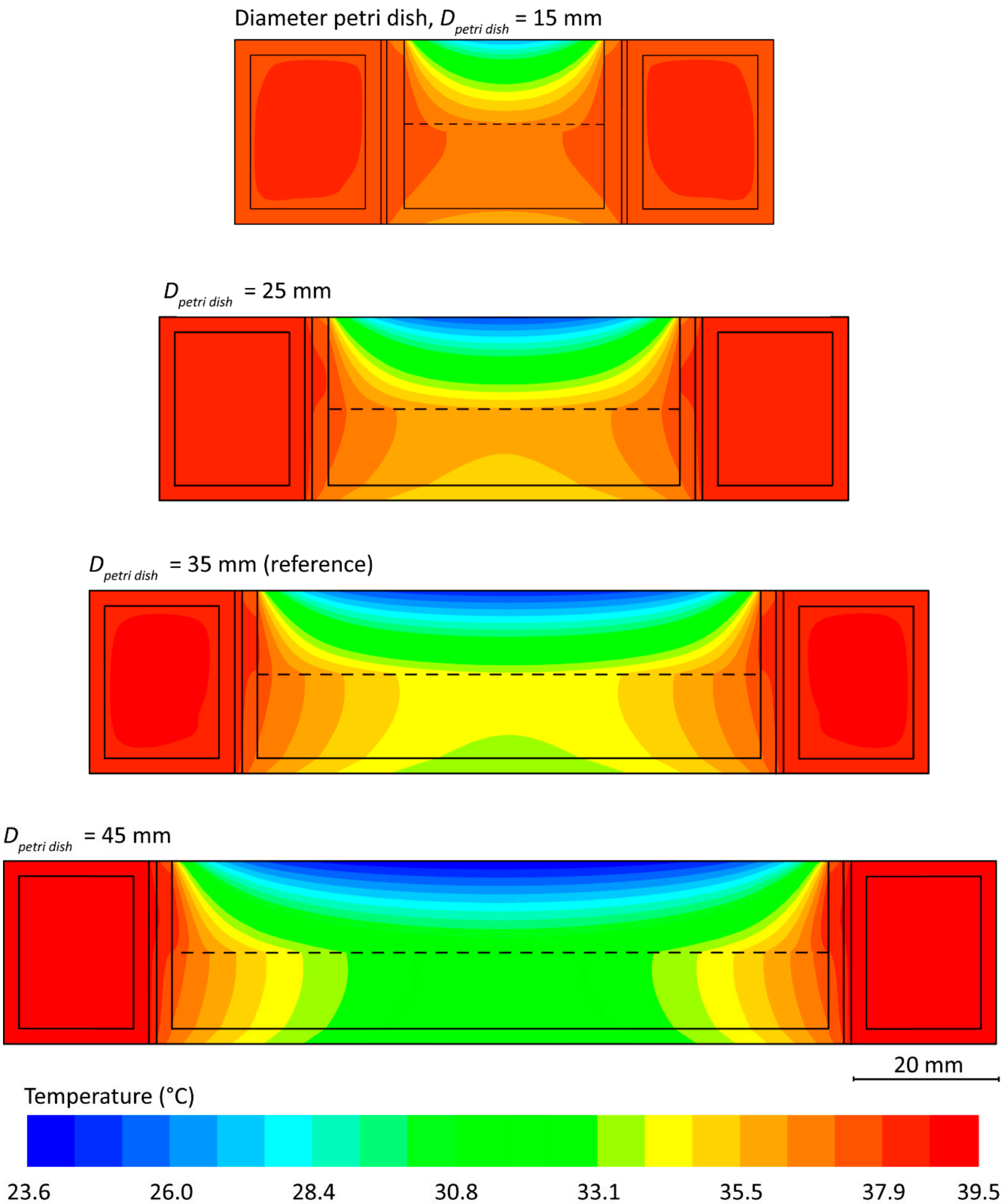

Figure S6. Characterizing the thermal performance of the water jacket system with respect to Petri dish diameter ($D_{Petri\ dish}$). The above contours show the temperature distribution along the middle cross section of the Petri dish for $D_{Petri\ dish}$ values of 15, 25, 35, and 45 mm, as discussed in **Figure 4a**.

Supplementary Information 8: Effect of sample volume inside the Petri dish

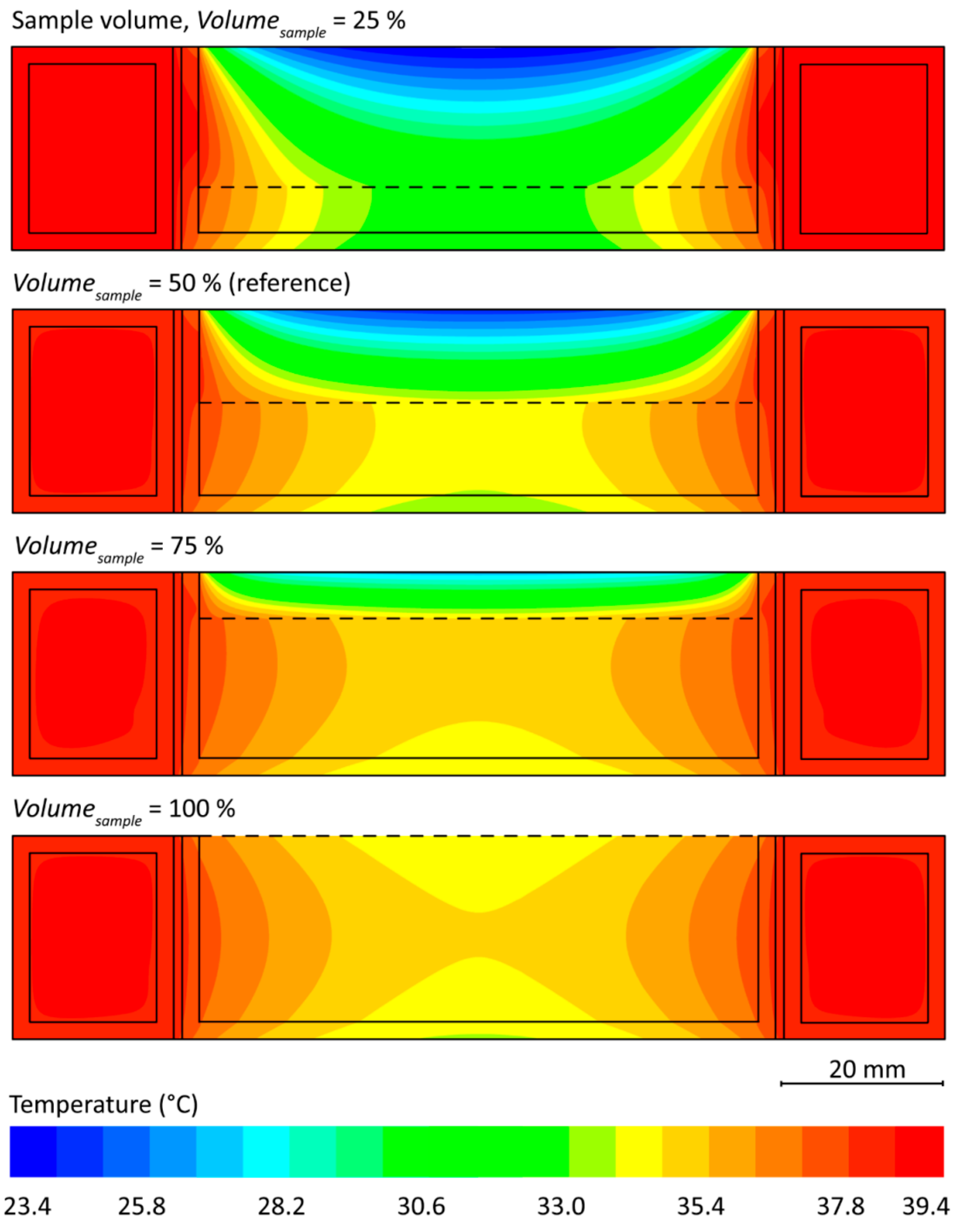

Figure S7. Characterizing the thermal performance of the water jacket system with respect to the volume of biological sample added into the Petri dish (V_{sample}). The above contours show the temperature distribution along the middle cross section of the Petri dish for V_{sample} values of 25, 50, 75, and 100%, as discussed in **Figure 4b**. The filled level of the sample inside the Petri dish is shown by dashed line.

Supplementary Information 9: Effect of Petri dish material

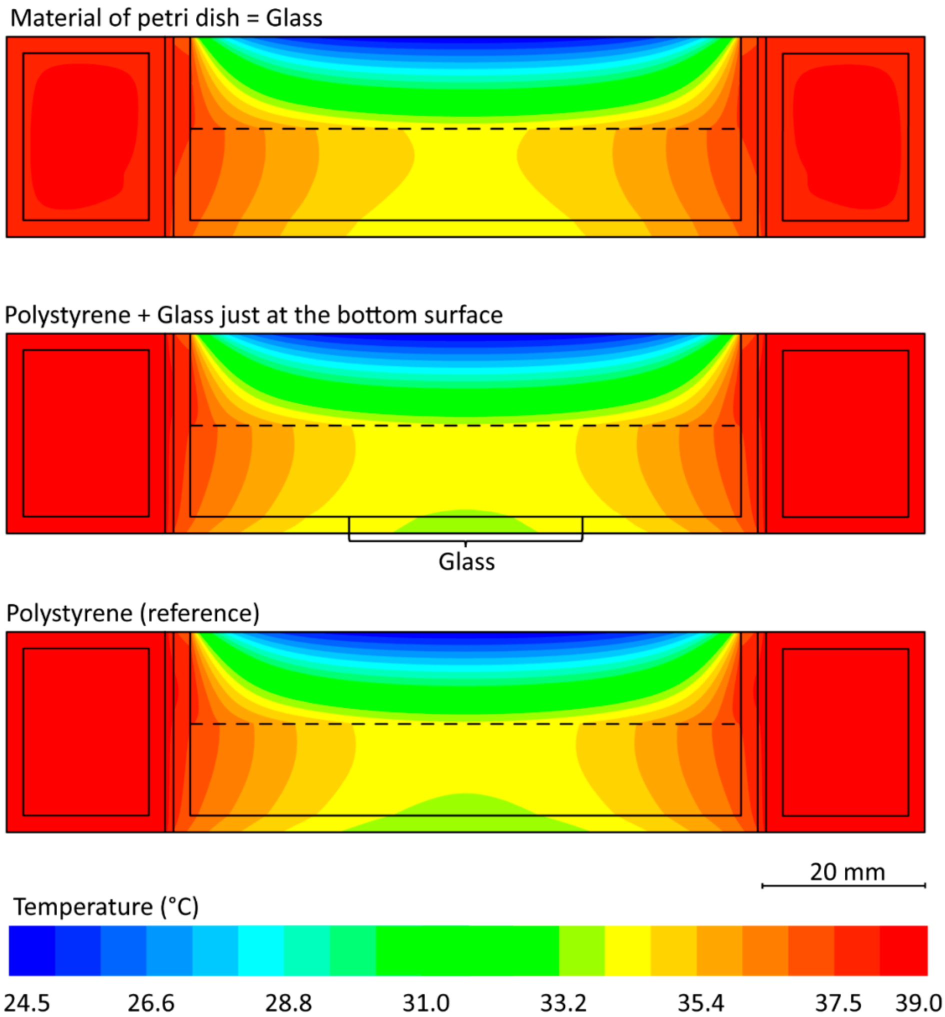

Figure S8. Characterizing the thermal performance of the water jacket system with respect to the material of Petri dish. The above contours show the temperature distribution along the middle cross section of the Petri dish for the cases of fully polystyrene, polystyrene-glass, and fully glass, as discussed in **Figure 4c**.

Supplementary Information 10: Effect of integrated heater

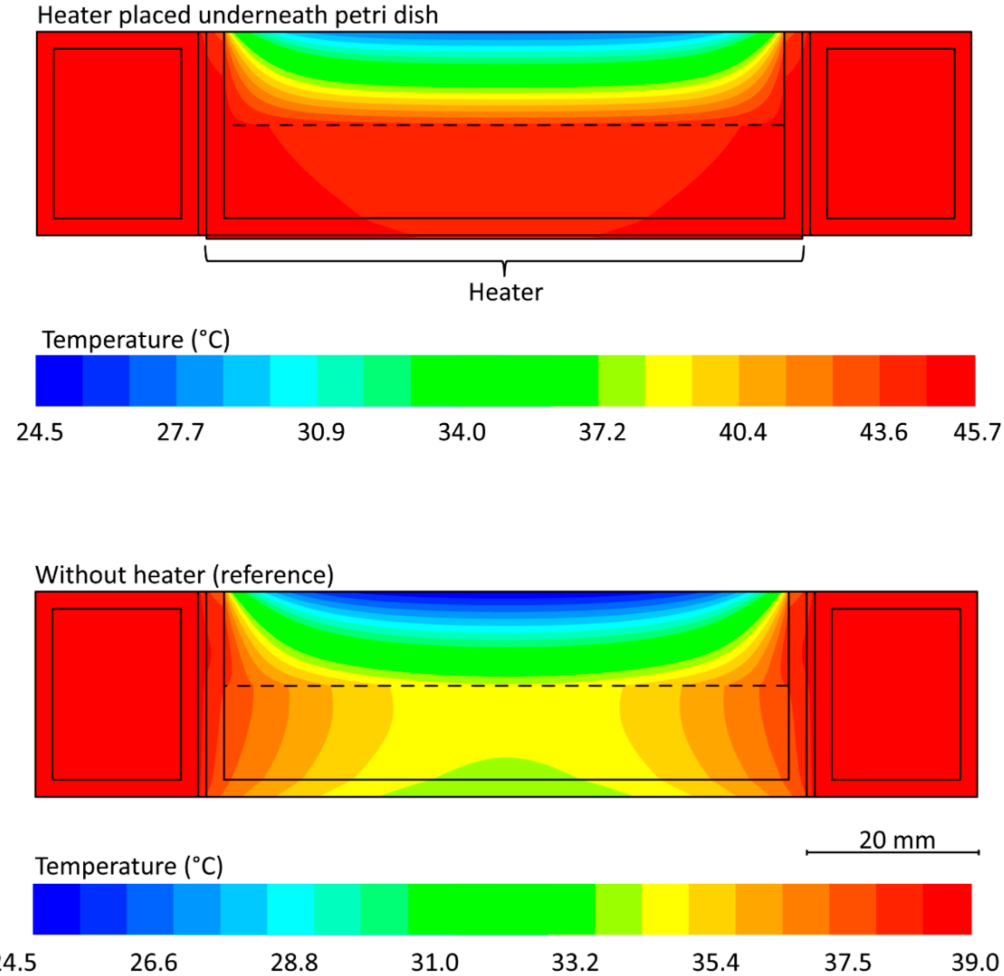

Figure S9. Characterizing the thermal performance of the water jacket system in the presence of a heater implemented underneath the Petri dish. The above contours show the temperature distribution along the middle cross section of the Petri dish in the absence and presence of a heater producing 187 mW, as discussed in **Figure 4d**.

Supplementary Information 11: Flow streamlines for square water jacket

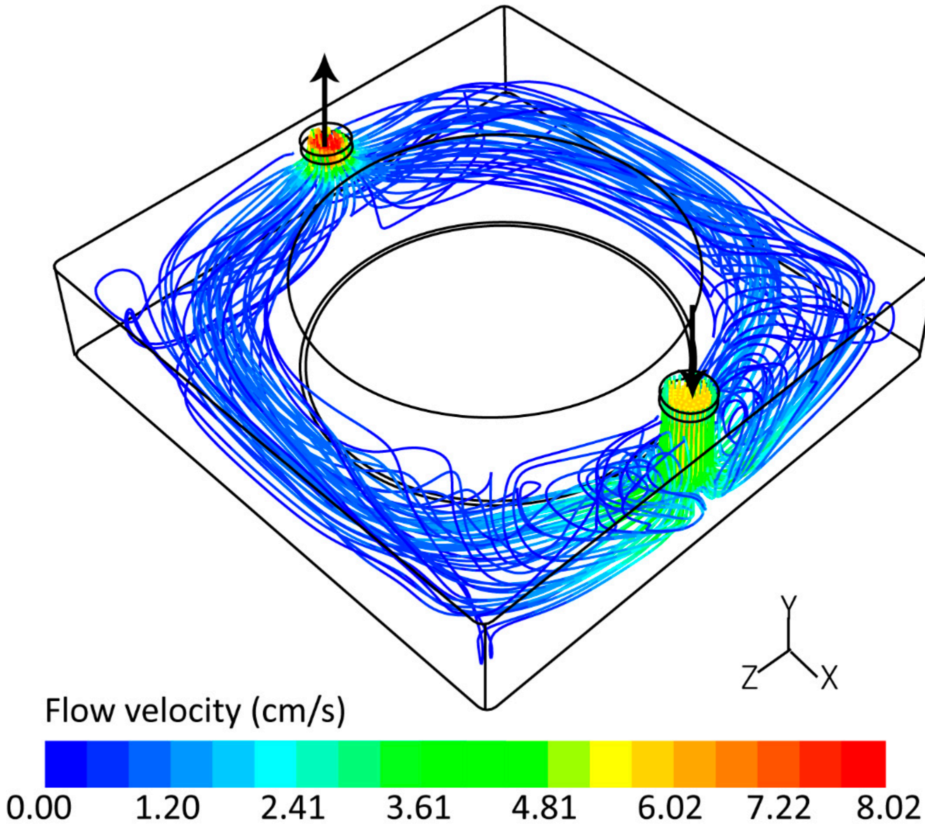

Figure S10. Flow streamlines along the square water jacket chamber coloured by velocity magnitude (cm/s), water is applied into the chamber at 60 mL/min, as discussed in **Figure 5a**.

Supplementary Information 12: Flow streamlines for semi-circular water jacket

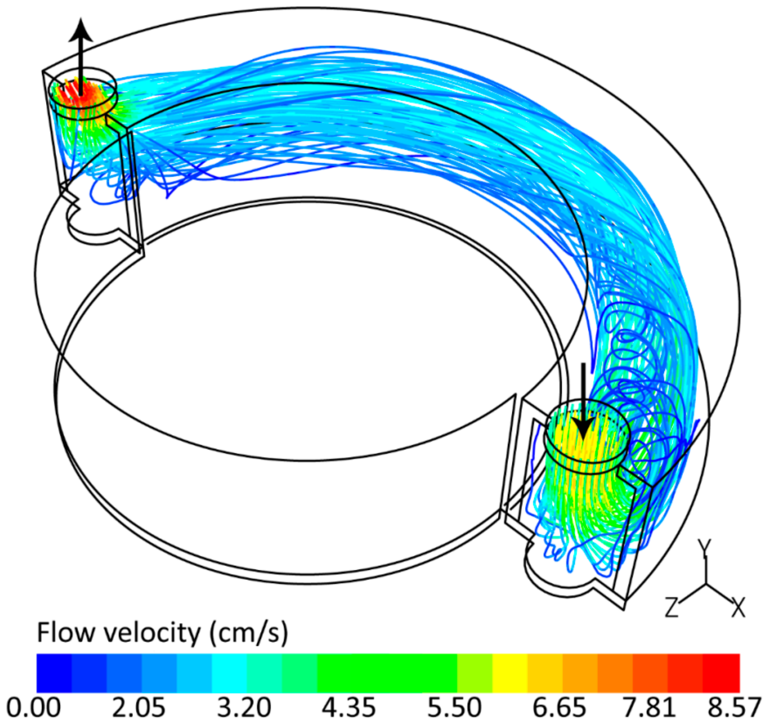

Figure S11. Flow streamlines along the semi-circular water jacket chamber coloured by velocity magnitude (cm/s), water is applied into the chamber at 60 mL/min, as discussed in **Figure 5b**.

Supplementary Information 13: Effect of microscopic stage

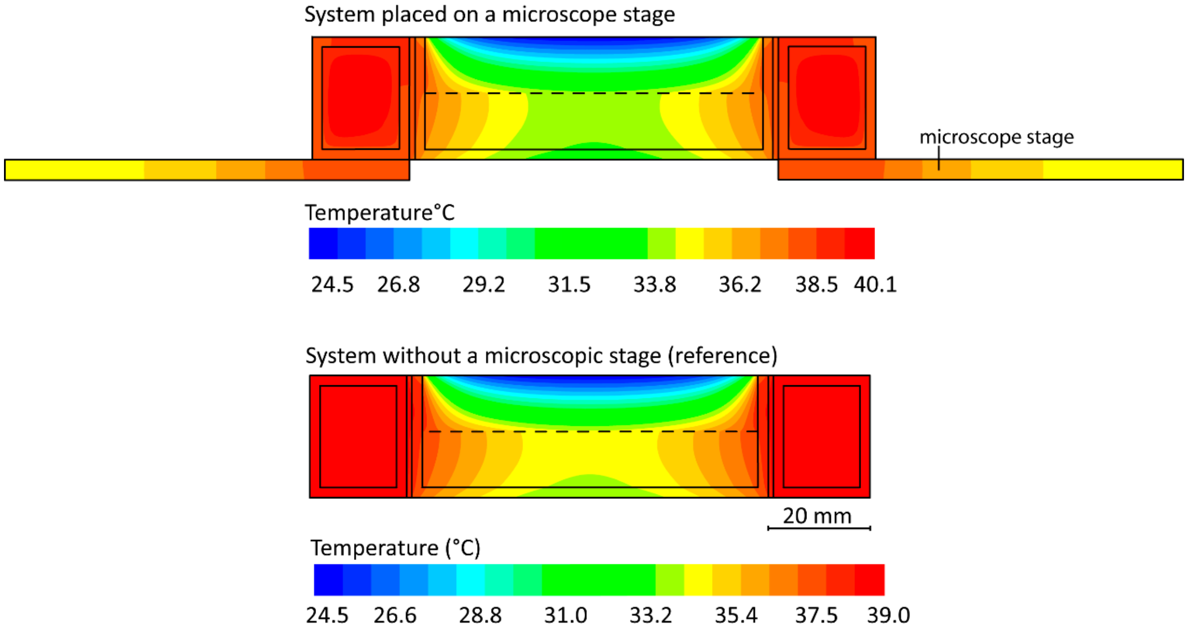

Figure S12. Characterizing the thermal performance of the water jacket system in the presence of a microscopic stage made of stainless steel with a thermal conductivity of 16.5 W/mK. The above contours show the temperature distribution along the middle cross section of the Petri dish in the absence and presence of a microscopic stage made of stainless steel with internal and external diameters of 36 and 115 mm and a thickness of 2 mm.

Supplementary Information 14: Effect of washer material

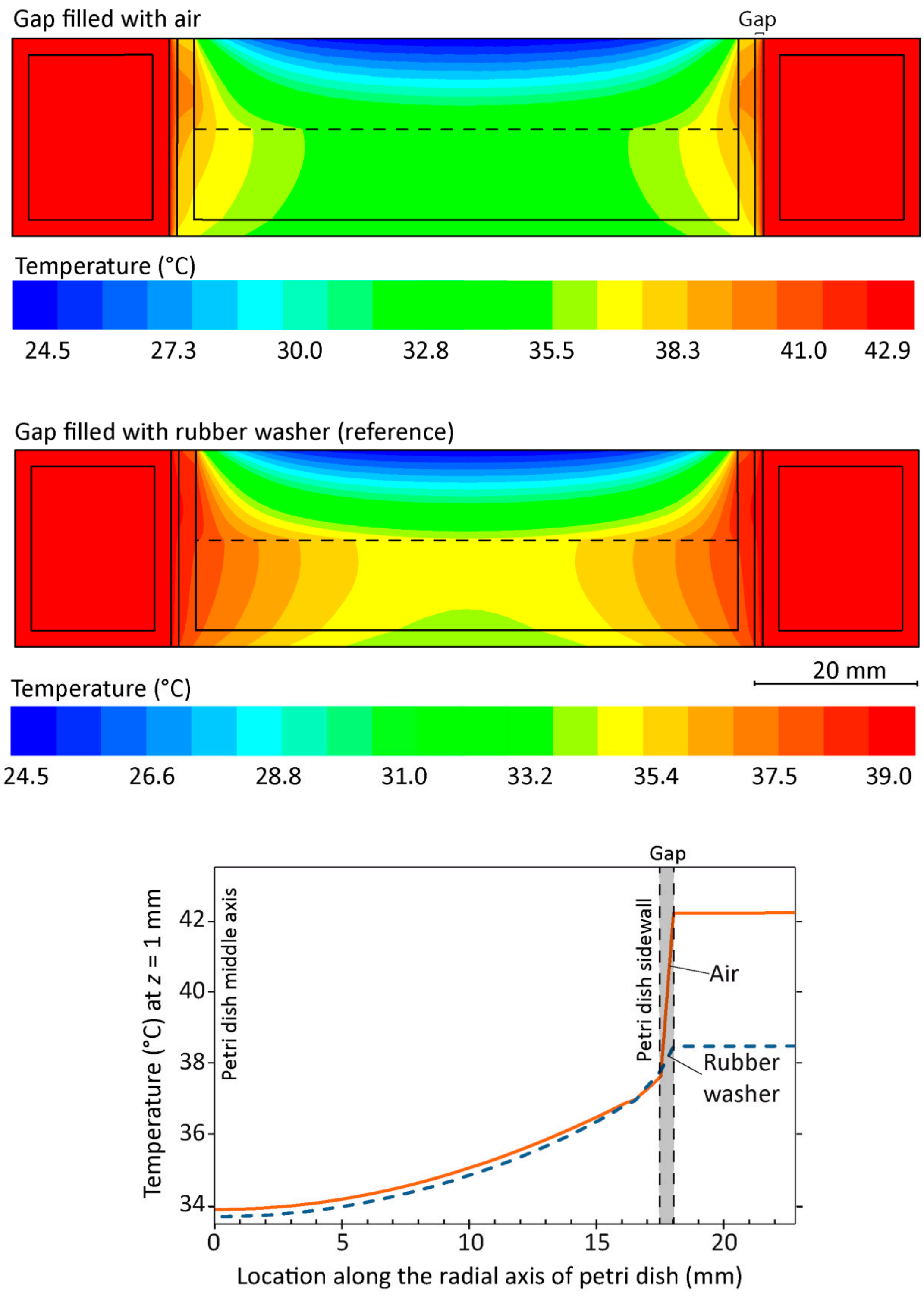

Figure S13. Characterizing the thermal performance of the water jacket system with respect to the material inserted between the Petri dish and the water jacket. The above contours show the temperature distribution along the middle cross section of the Petri dish for the cases of air and rubber washer. The plot compares the temperature profile along the radial axis of the Petri dish.

Supplementary Information 15: Effect of Petri dish lid

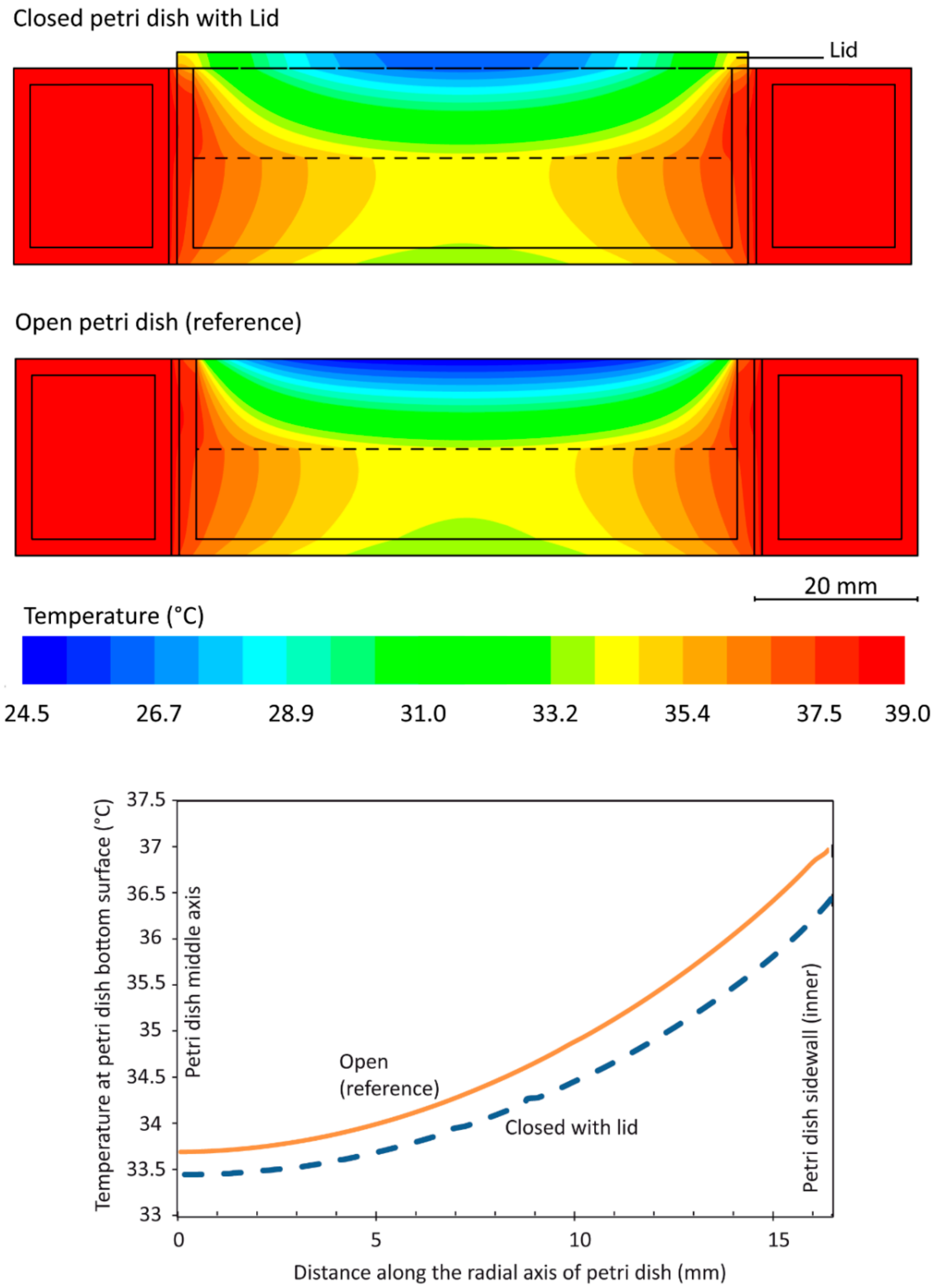

Figure S14. Characterizing the thermal performance of the water jacket system in the presence of a polystyrene lid inserted on the top surface of the Petri dish. The above contours show the temperature distribution along the middle cross section of the Petri dish in the presence and absence of the polystyrene lid. The plot compares the temperature profile along the radial axis of the Petri dish in the presence and absence of the lid.

Supplementary Information 16: Transient response for increasing target sample temperature from 37 to 45°C

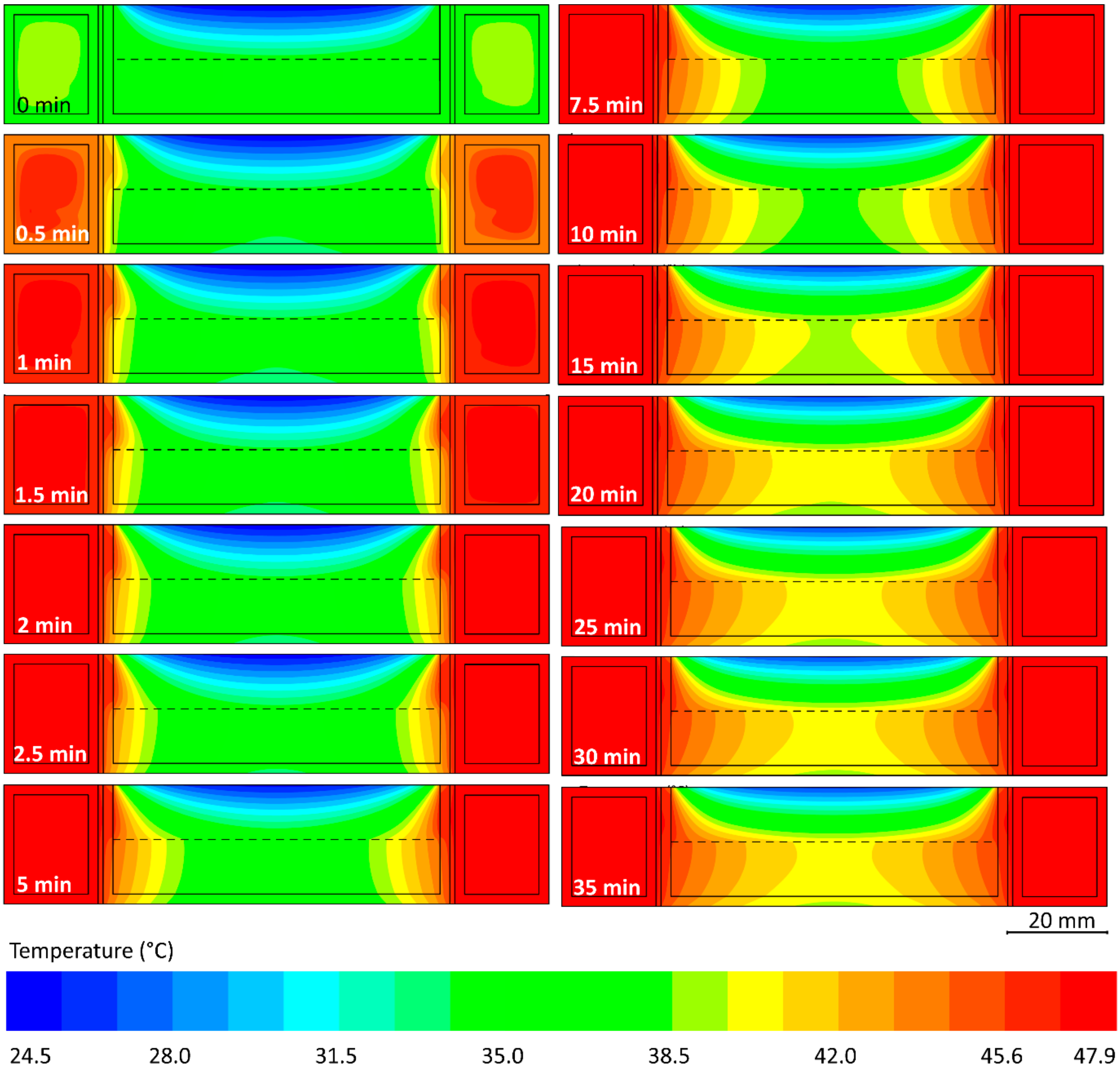

Figure S15. Characterizing the dynamic response of the water jacket system when increasing the water inlet temperature from **39.0 to 48.5°C** at 0 min (corresponding to varying the target sample temperature from 37 to 45°C), as discussed in **Figures 7b-d**.

Supplementary Information 17: Transient response for increasing target sample temperature from 37 to 42°C

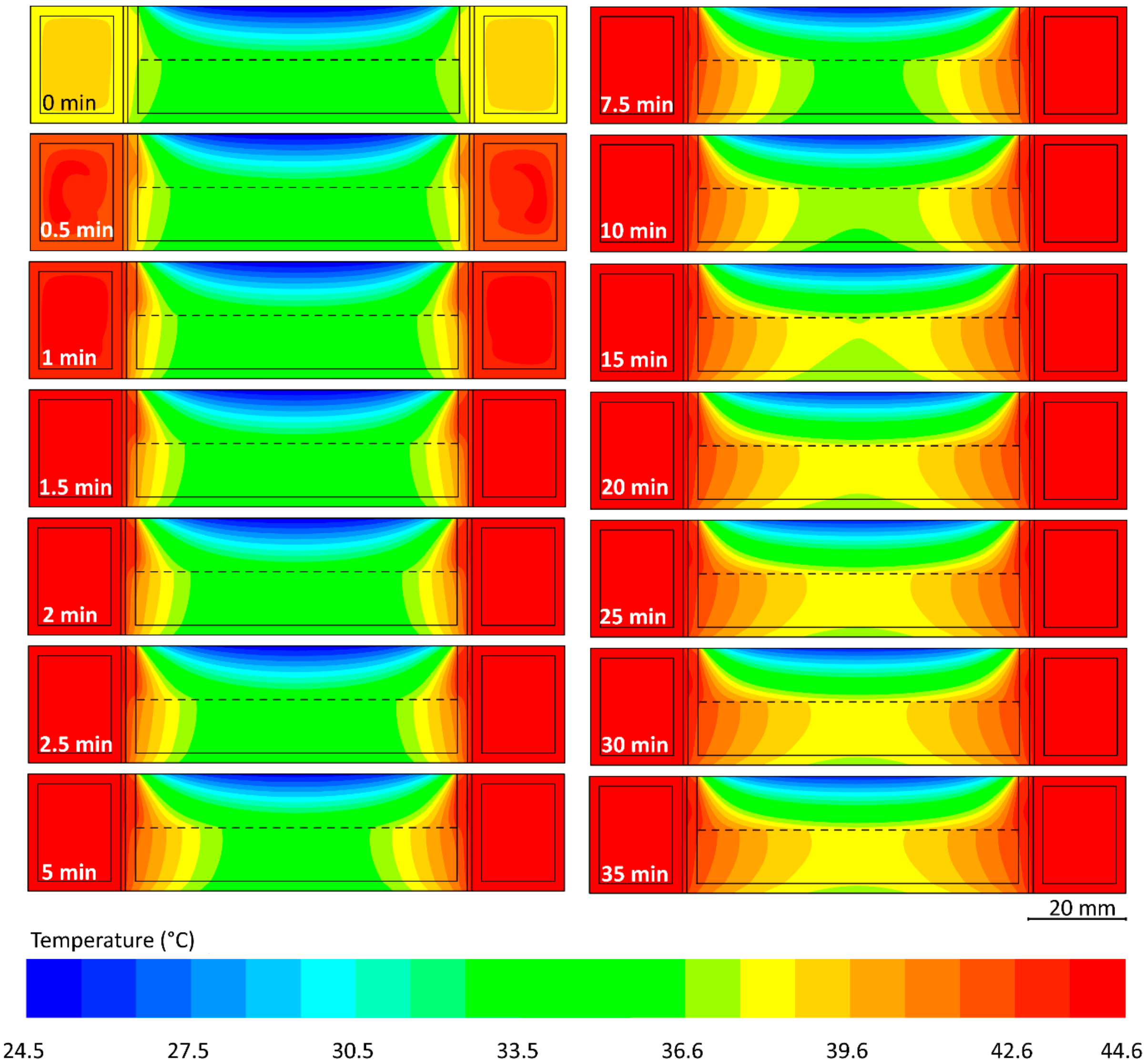

Figure S16. Characterizing the dynamic response of the water jacket system when increasing the water inlet temperature from **39.0 to 44.6°C** at 0 min (corresponding to varying the target sample temperature from 37 to 42°C), as discussed in **Figure 7e.**

Supplementary Information 18: Transient response for decreasing target sample temperature from 37 to 25°C

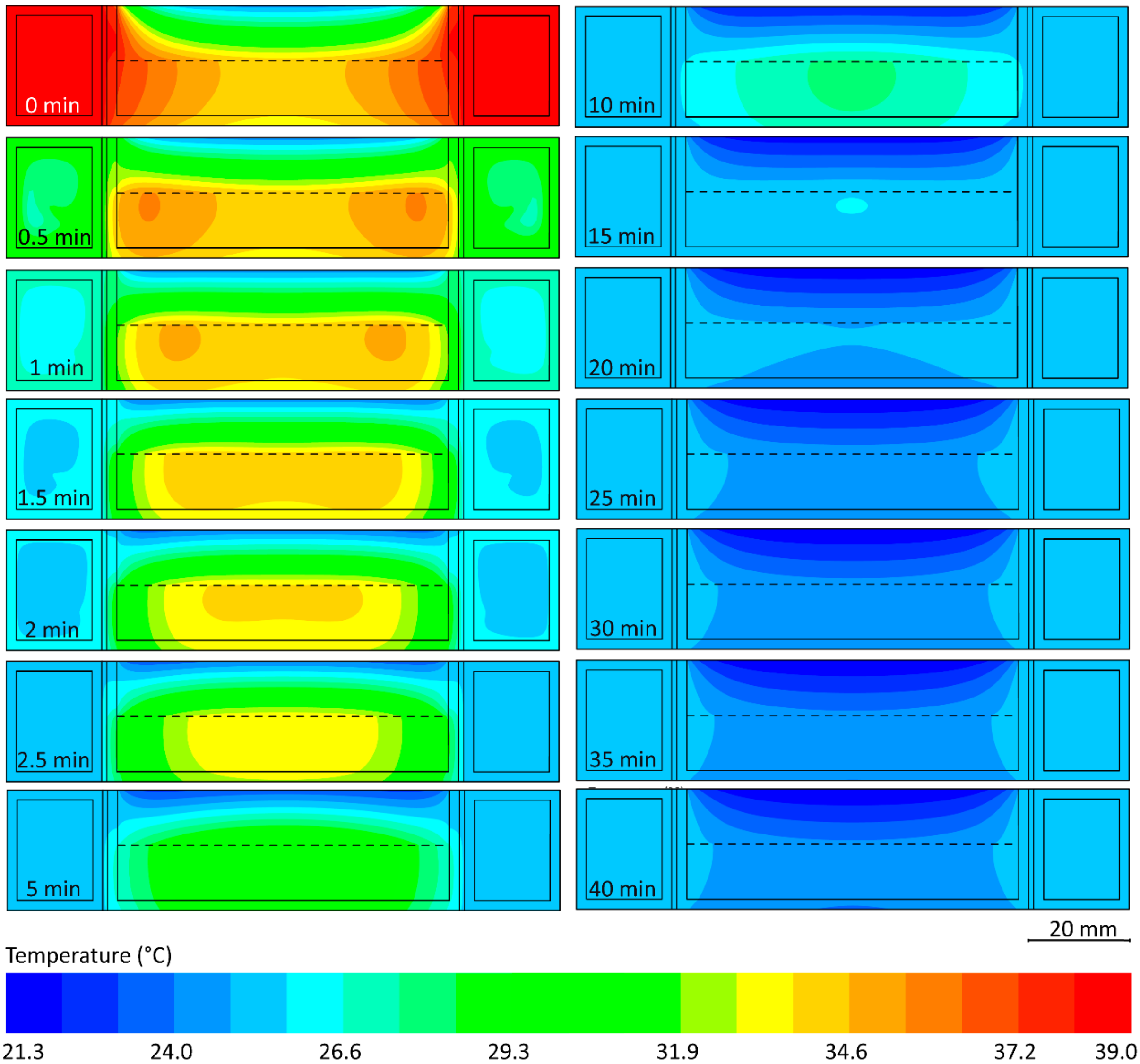

Figure S17. Characterizing the dynamic response of the water jacket system when decreasing the water inlet temperature from **39 to 25.55°C** at 0 min (corresponding to varying the target sample temperature from 37 to 25°C), as discussed in **Figure 7e**.

Supplementary Information 19: Transient response for decreasing target sample temperature from 37 to 15°C

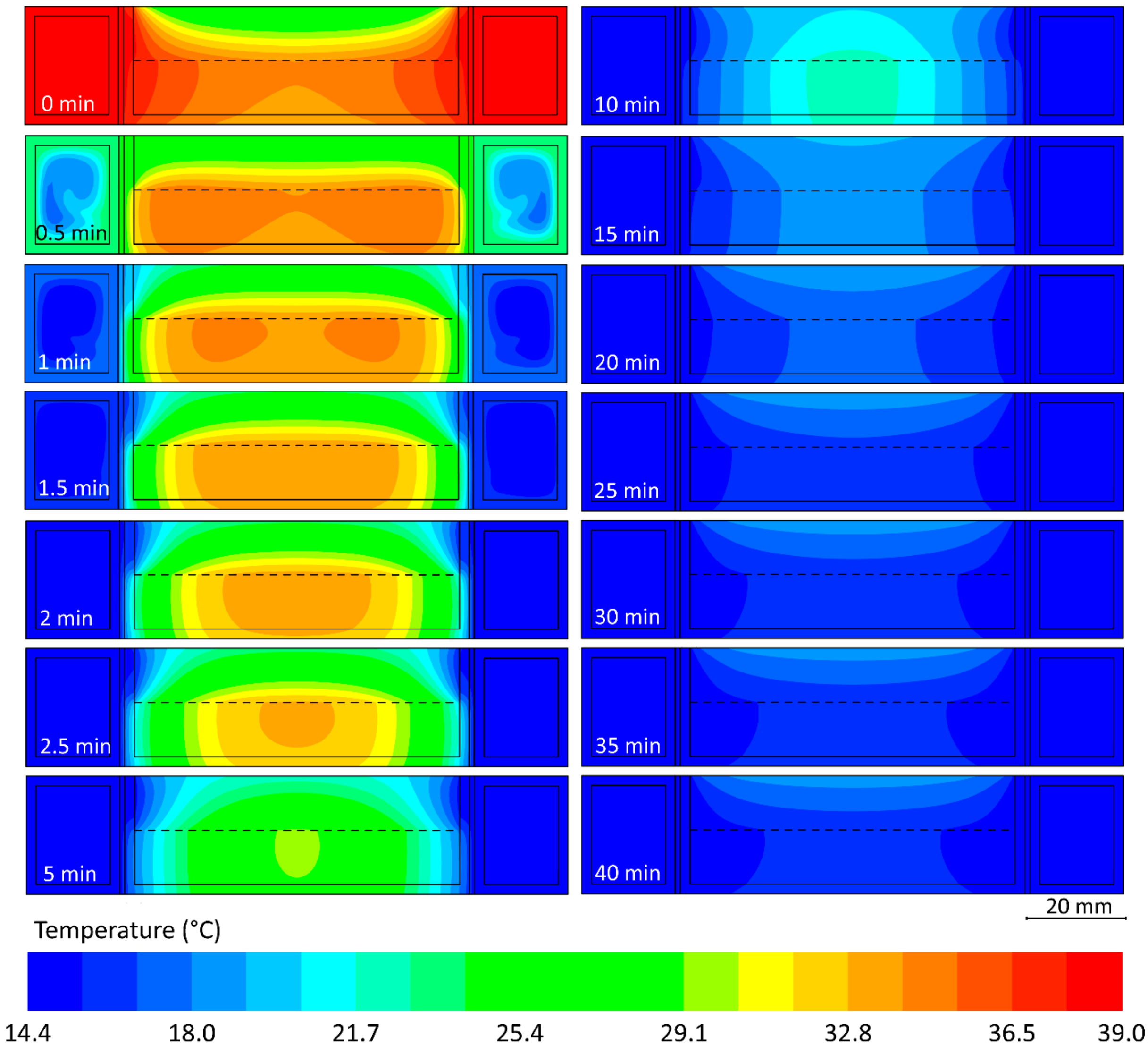

Figure S18. Characterizing the dynamic response of the water jacket system when decreasing the water inlet temperature from **39 to 14.35°C** at 0 min (corresponding to varying the target sample temperature from 37 to 15°C), as discussed in **Figure 7e**.

Supplementary Information 20: Transient response for increasing target sample temperature from 37 to 45°C at increased water flow rate of 120 mL/min

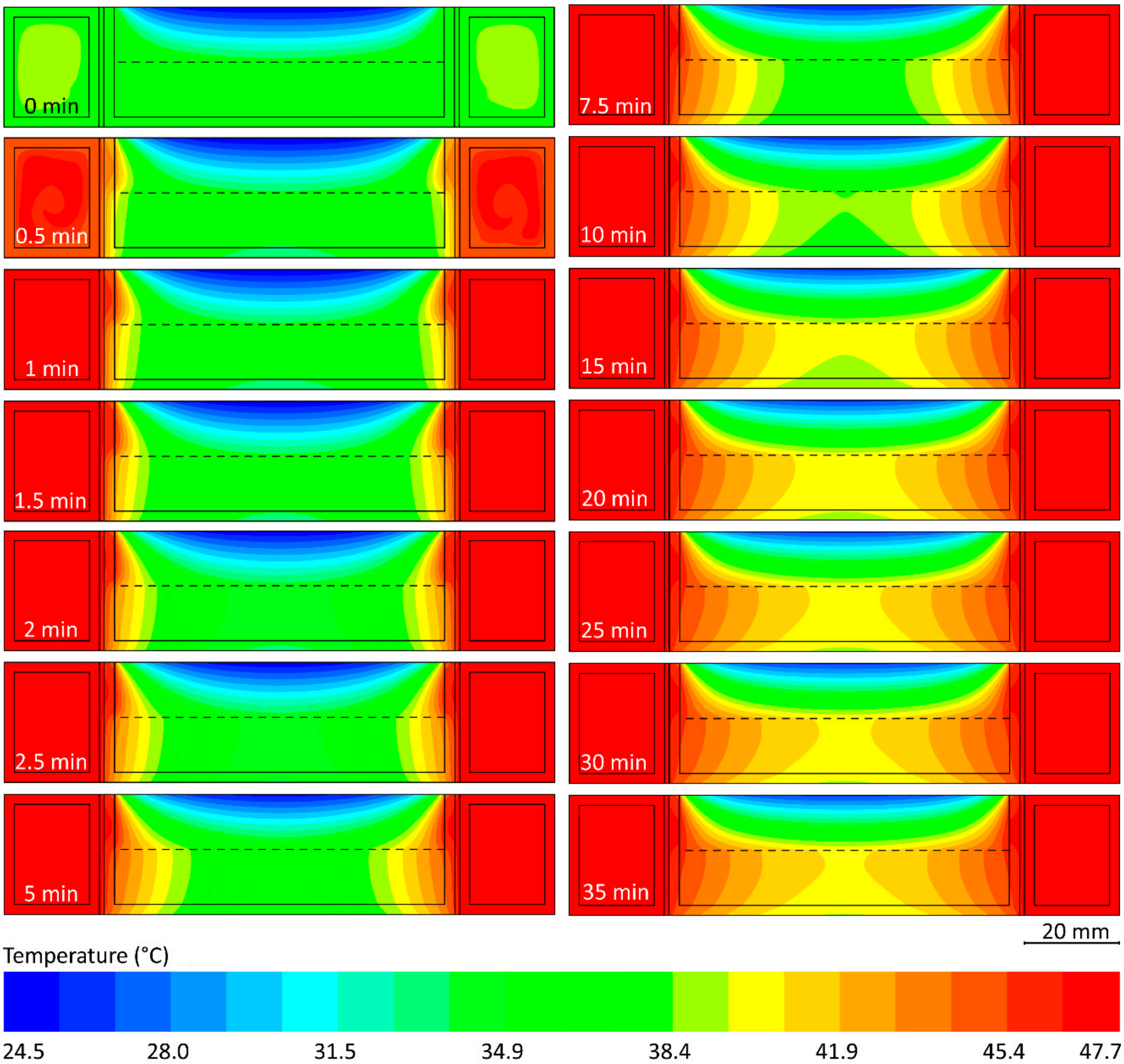

Figure S19. Characterizing the dynamic response of the water jacket system when increasing the water inlet temperature from 39 to 47.7°C at 0 min (corresponding to varying the target sample temperature from 37 to 45°C) at a water flow rate of 120 mL/min recirculating through the water jacket), as discussed in **Figure 8b**.

.

Supplementary Information 21: Transient response for increasing target sample temperature from 37 to 45°C for a Petri dish diameter of 15 mm

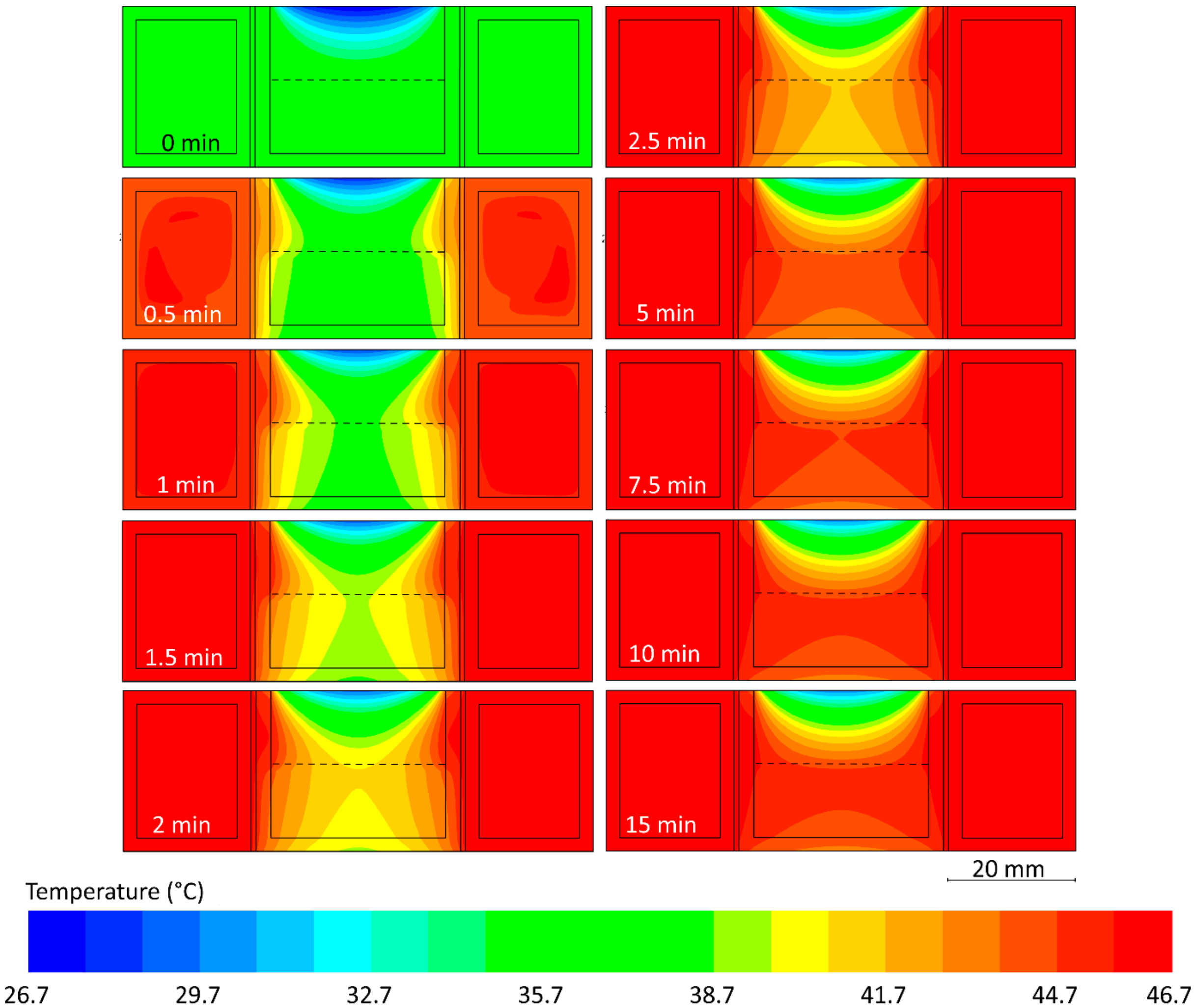

Figure S20. Characterizing the dynamic response of the water jacket system with a **Petri dish diameter of 15 mm** when increasing the water inlet temperature from 39 to 46.7°C at 0 min (corresponding to varying the target sample temperature from 37 to 45°C), as discussed in **Figure 8c**.

Supplementary Information 22: Transient response for increasing target sample temperature from 37 to 45°C for a Petri dish diameter of 25 mm

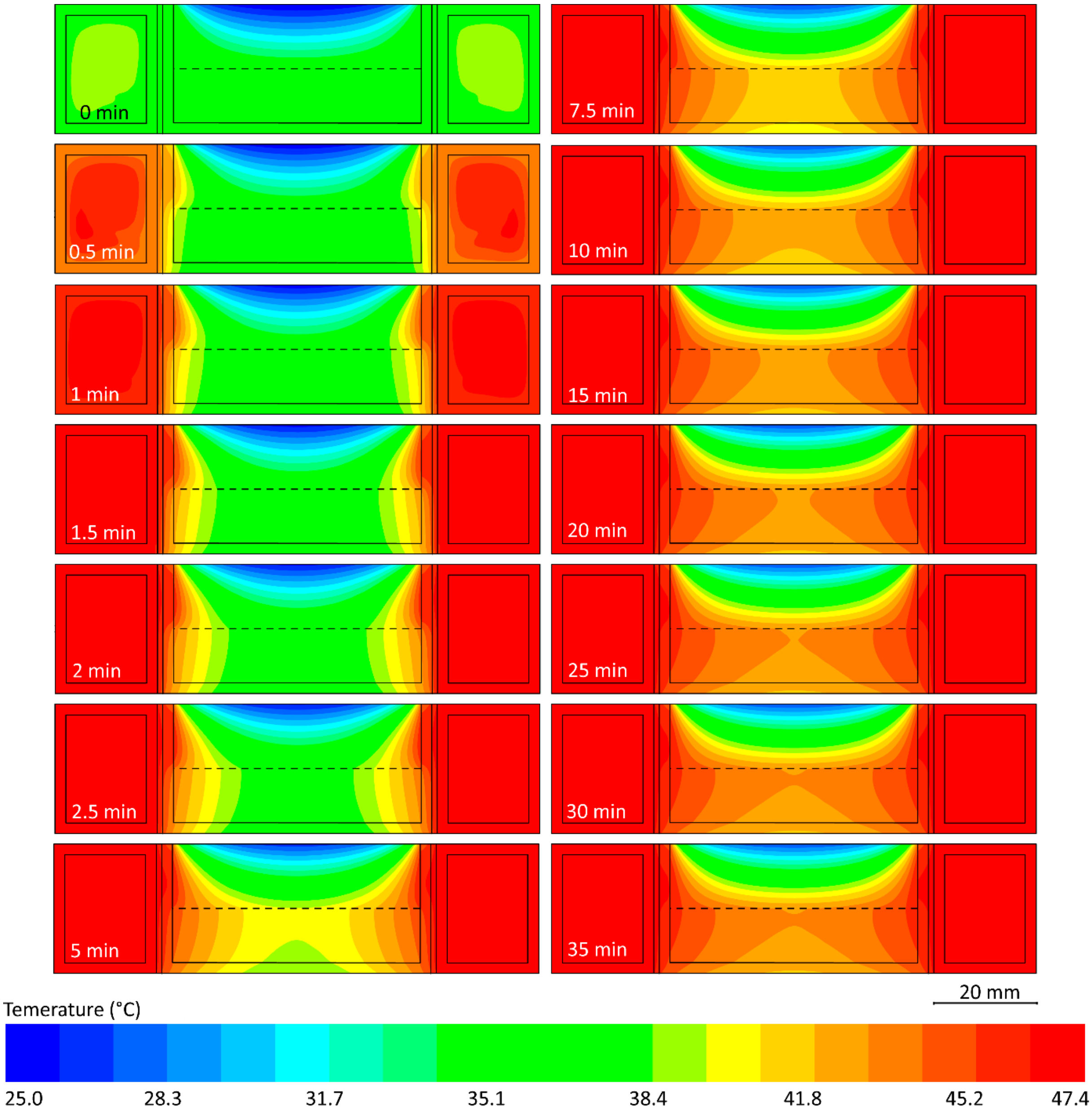

Figure S21. Characterizing the dynamic response of the water jacket system with a **Petri dish diameter of 25 mm** when increasing the water inlet temperature from 39 to 47.4°C at 0 min (corresponding to varying the target sample temperature from 37 to 45°C), as discussed in **Figure 8c**.

Supplementary Information 23: Transient response for increasing target sample temperature from 37 to 45°C for a sample volume of 25%

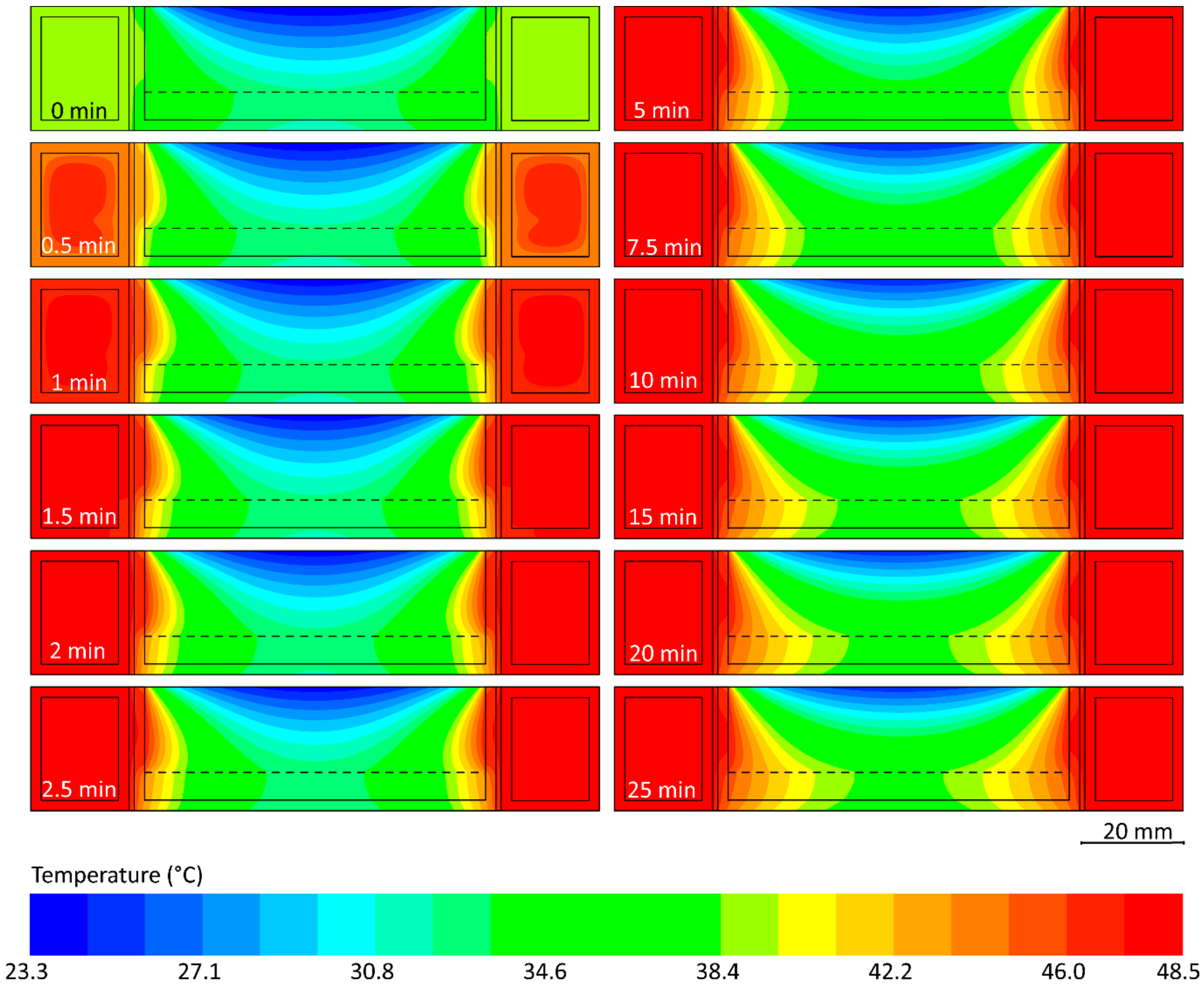

Figure S22. Characterizing the dynamic response of the water jacket with a **sample volume of 25%** inside the Petri dish (shown with dashed line) when increasing the water inlet temperature from 39 to 48.5°C at 0 min (corresponding to varying the target sample temperature from 37 to 45 C), as discussed in **Figure 8d**.

Supplementary Information 24: Transient response for increasing target sample temperature from 37 to 45°C for a glass Petri dish

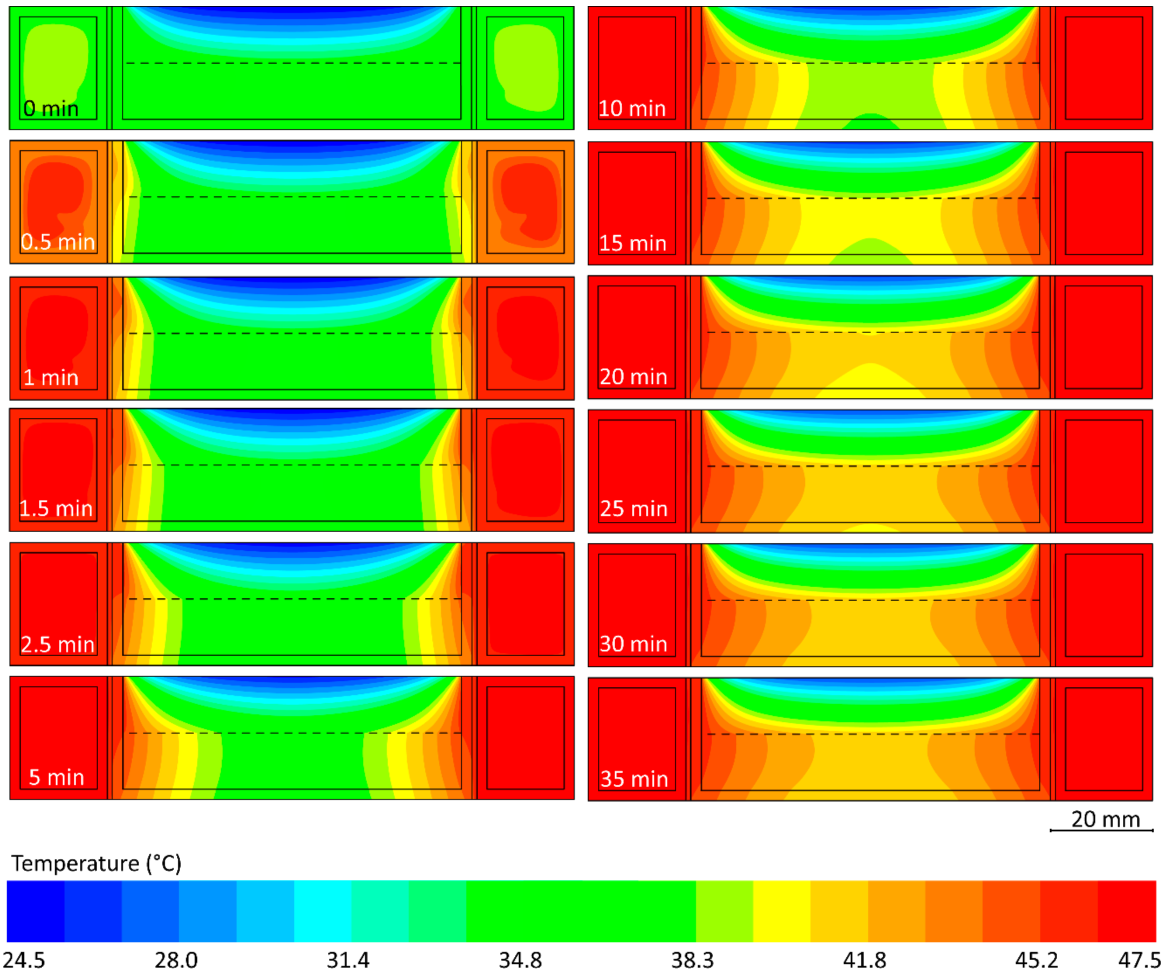

Figure S23. Characterizing the dynamic response of the water jacket with a **glass Petri dish** when increasing the water inlet temperature from 39 to 47.5°C at 0 min (corresponding to varying the target sample temperature from 37 to 45°C), as discussed in **Figure 8e**.

Supplementary Information 25: Transient response for increasing target sample temperature from 37 to 45°C for a glass Petri dish with an integrated heater

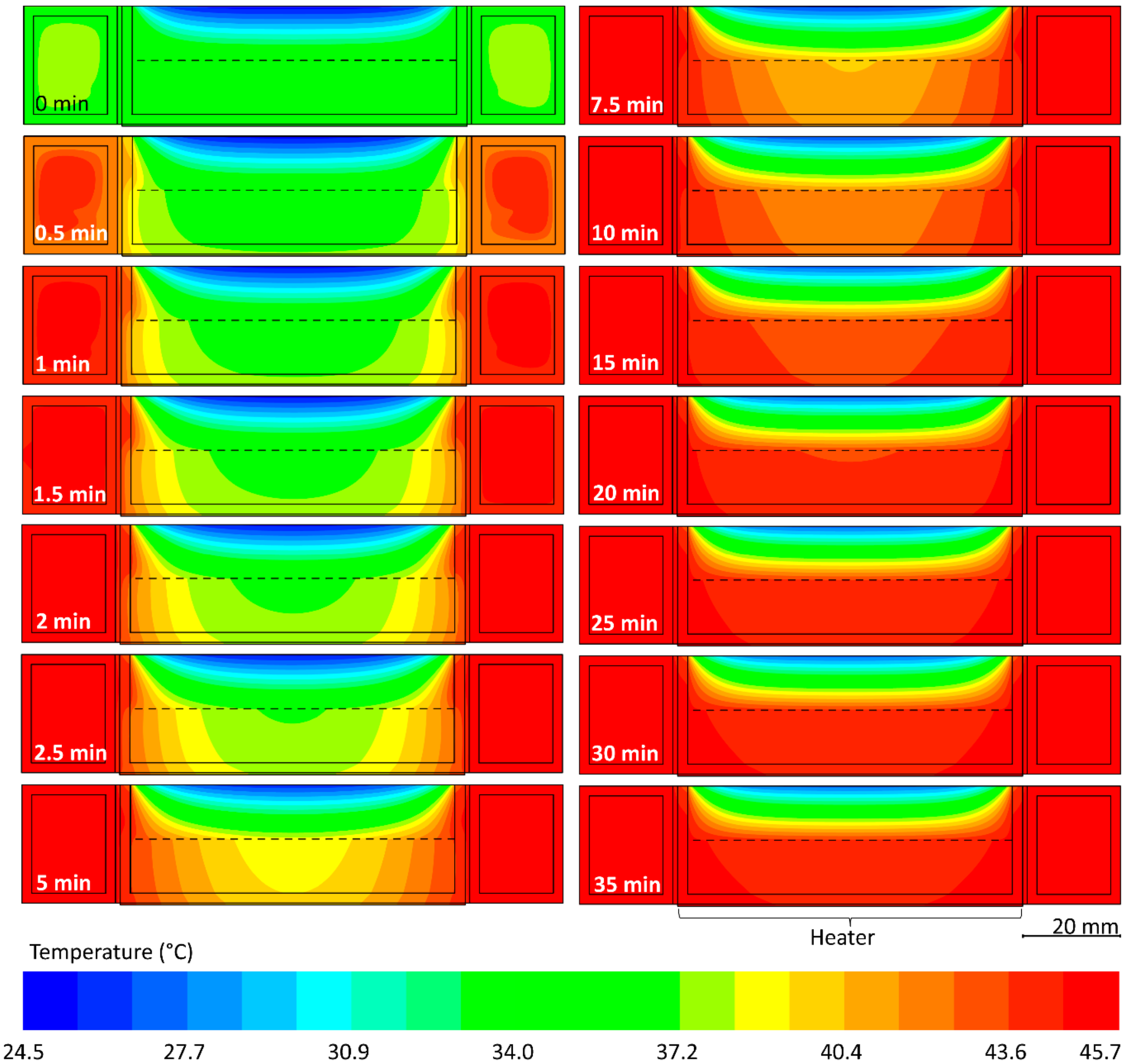

Figure S24. Characterizing the dynamic response of the water jacket with a **heater implemented underneath the Petri dish** producing 265 mW along with increasing the water inlet temperature from 39 to 45.7°C at 0 min (corresponding to varying the target sample temperature from 37 to 45°C), as discussed in **Figure 8f**.

Supplementary Information 26: Transient response for decreasing target sample temperature from 37 to 29°C for a localised heat transfer coefficient of 20 W/m^2K

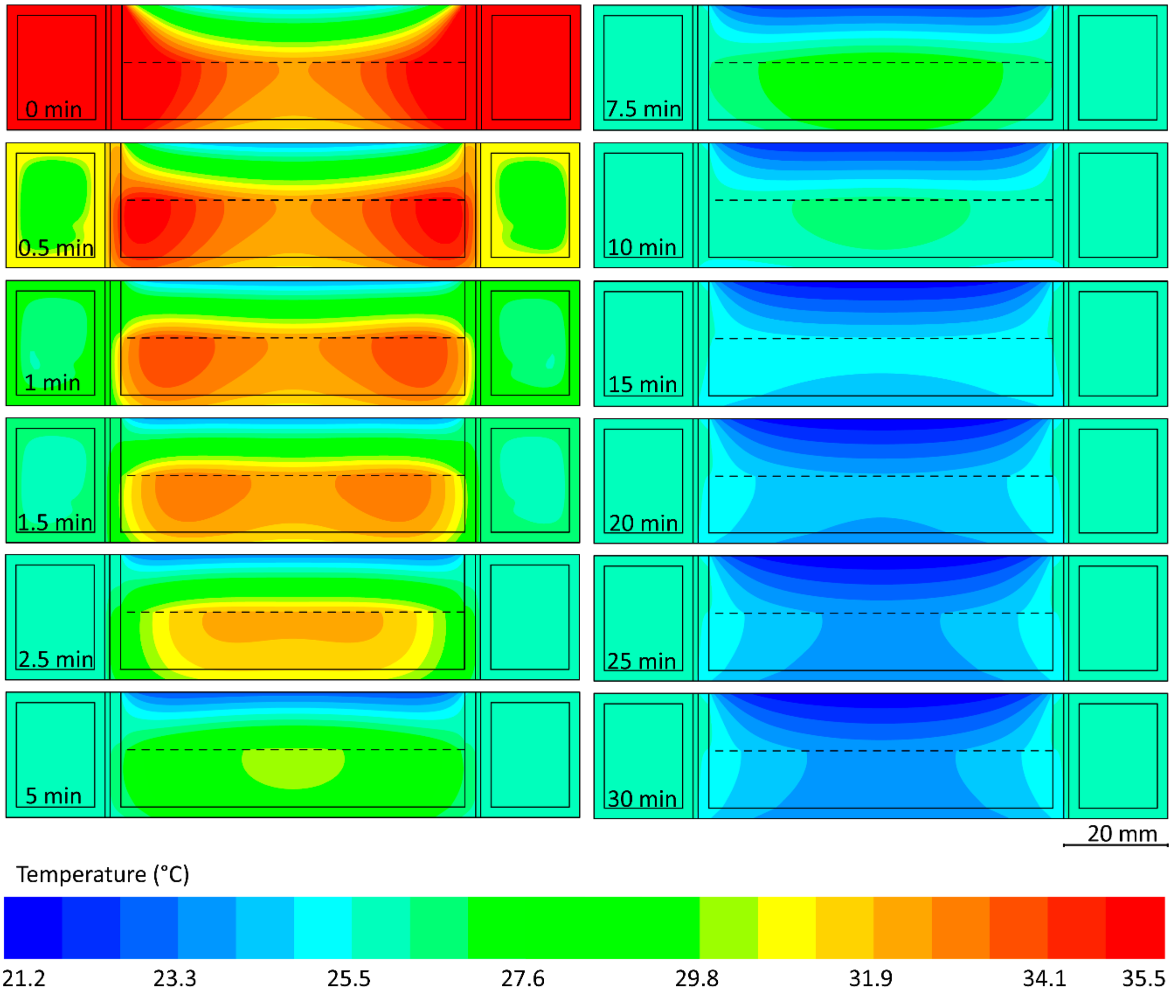

Figure S25. Characterizing the dynamic response of the water jacket by setting the localised heat transfer coefficient at the bottom surface of the Petri dish bottom to 20 W/m^2K along with decreasing the water inlet temperature from 39 to 30.7°C at 0 min (corresponding to varying the target sample temperature from 37 to 29°C), as discussed in **Figure 8g**.